**Accepted for publication in Journal of Reinforced Plactics and Composites**
**Published in 2016**
**DOI: 10.1177/0731684416665176**

# Low-cycle fatigue properties of basalt fiber and graphene reinforced polyamide 6 hybrid composites

László Mészáros [a,b,*], József Szakács [a]

[a] Department of Polymer Engineering, Faculty of Mechanical Engineering, Budapest University of Technology and Economics, Muegyetem rkp. 3., H-1111 Budapest, Hungary

[b] MTA–BME Research Group for Composite Science and Technology, Muegyetem rkp. 3., H-1111 Budapest, Hungary

[*] corresponding author, e-mail: meszaros@pt.bme.hu,

Phone: +36-1-463-3083

Fax: +36-1-463-1527

keywords: polyamide 6, graphene, fatigue, hybrid composites, basalt fiber

## Abstract

In this study the effect of graphene content on quasi-static and fatigue mechanical properties of basalt fiber reinforced polyamide 6 is investigated. Hybrid composites and reference monocomposites were melt compounded, then specimens were injection molded. Although the presence of graphene caused moderate change in quasi-static tensile properties, remarkable increment in the fatigue properties of hybrid composites was experienced. Hybrid composites

with low graphene content withstood higher number of cycles in fatigue tests at the same loading compared to basalt fiber reinforced monocomposites. Scanning electron microscopy of the fracture surfaces revealed proper dispersion of reinforcement in the hybrid materials, an explanation to the better fatigue performance at lower graphene contents.

## 1. Introduction

Performance improvement is one of the most important criteria when a novel polymer composite is developed for engineering applications. Although traditional, two-phase composites are still being developed, more and more researchers think that using an additional third phase might be an effective way to increase the mechanical performance of a composite or endow it with functional properties. This third phase can be another matrix or a reinforcing material. In the first case the main goal is often to create a co-continuous phase and this way energy consumption during fracture process could be enhanced. In the second case, where two different reinforcing materials are present, the aim is to increase the strength and the stiffness of the material. Besides microfibers various types of nanoparticles are widely applied as secondary reinforcing materials [1 - 6].

In the last decade the appearance of graphene presented challenges for researchers in the field of composites, too. Beside the unique electrical and thermal properties, graphene has the greatest tensile strength and modulus among the known materials and it has extremely high aspect ratio [7 - 12]. These superior properties make graphene a prominent alternative to increase the mechanical performance of polymers [13 - 15]. Due to its high specific surface graphene especially tends to form aggregates, and that causes difficulties in the preparation of nanocomposites with graphene content. There are several methods developed for breaking up these aggregates, but the main problem is that they cannot often be adapted to industrial purposes [16].

A solution for the above mentioned problems could be if the three raw materials (nanoparticles, microparticles and the matrix) are melt mixed together. Besides its simplicity, the main benefit of this process is that the presence of microfibers in the polymer melt increases apparent viscosity, therefore higher shear forces arise during processing, and this way better nanoparticle dispersion can be achieved [17 - 20].

The positive effects of conventional fiber reinforcement on fatigue properties of polymers are well known and deeply examined. More and more researchers think that at a fatigue test not just the fatigue life of a material is important but also the failure process itself, therefore researchers pay more attention to the investigation of fatigue crack propagation and failure analysis [21 - 26].

The test parameters and conditions can also change the fatigue behavior of polymers, which is especially true for polyamides. For instance as polyamides are hydrophilic materials and the amount of the absorbed water affects the mechanical properties, therefore the water content also has significant impact on the fatigue properties [26]. The loading force applied during the fatigue test also change the cycle number connected the failure. The fatigue life is can also be connected to the temperature and the modulus of the material as Esmaelliou *et al.* [27] demonstrated for glass fiber reinforced polyamide matrix composites. They found that the fatigue process during loading of polyamides can be divided into three parts. In the first part the relative Young's modulus decreases intensively and temperature increases gradually until it exceeds the glass transition temperature of the material. Then in the second part, both the temperature and the relative modulus are approximately constant. In the third part temperature increases and relative modulus decreases again until failure. At higher load levels the second and the third part become less remarkable and gradually disappear by further load increment. This is why it is important to choose appropriate loads and to make thermal investigation of the material during a fatigue test.

There are several studies about the effect of nanoparticles on fatigue properties. Generally it can be stated that if adhesion between the matrix and nanoparticles is proper, nanoparticles can hinder crack propagation, and as a result longer fatigue life is achieved [28, 29]. For instance Loos *et al.* [29] found that fatigue life of carbon nanotube (CNT) reinforced epoxy composite is higher than that of the neat matrix at each load level applied. Scanning electron micrographs indicated that the key mechanism of enhanced fatigue life is crack-bridging and pull-out mechanism of CNTs, as these phenomena increase the absorbed energy during the fracture process.

The fatigue properties of hybrid composites are less investigated, however there are some studies about the positive effects of reinforcing material hybridization on the fatigue behavior of composites [30-32]. From the quasi-static mechanical properties point of view it is acknowledge that the nanoparticles increase the strength and the modulus of hybrid composites. Beside the fact that the nanoparticles themselves can change the performance of the matrix they can act as stress distributors. Another studies explain the increased mechanical performance by that the nanoparticles appear in the microfiber-matrix boundary phase and help in the stress transfer between the phases Whichever mode of action is dominant the results should be appeared also in increased fatigue properties [33-36].Grimmer *et al.* [30] investigated the fatigue life of carbon nanotube and glass fiber reinforced epoxy matrix hybrid composites. The presence of a relatively low amount of carbon nanotubes reduced cyclic delamination and crack propagation in the material significantly. This effect was more remarkable at lower cyclic stress levels.

In one of our previous studies [37] the effects of graphene on the elastic properties of polyamide 6 were presented via a special cyclic test, where load was increased in every cycle. This test makes it relatively easy to determine the deformation components (residual and elastic) at different load levels. It was showed that the presence of graphene efficiently decreased the

residual deformation of nanocomposites at every load level, and that resulted in a higher rate of elastic recovery compared to the matrix material. As the presence of graphene increased the elasticity of the material, higher fatigue life could be expected not just for nano but also for hybrid composites.

The aim of the present study is to produce hybrid composites with graphene and basalt fiber content, and investigate their quasi-static mechanical and fatigue performance.

## 2. Materials and methods

### *2.1. Materials*

Schulamid 6 MV 13 type polyamide 6 (PA 6) from A. Schulman GmbH (Germany) was used as matrix material. BCS KV02 type basalt fiber with silane sizing (BF) from Kamenny Vek Ltd. (Russia) was applied as micro-sized reinforcement. The initial length of the fibers were 6 mm and average diameter was 15,6±1,9 μm. Graphene xGnP® Graphene Nanoplatelets - Grade H (GnP) supplied by XG Sciences, Inc. (USA) were used as nano-sized reinforcement. Nanoparticles had an average thickness of 15 nm and the average particle diameter was 25 μm.

### *2.2. Sample preparation*

A Labtech Scientific type twin screw extruder (L/D=44; D=26 mm) was used for continuous melt mixing. The screw speed was 25 1/min and the extrusion temperature was 250°C. For the different composites 30 wt% BF and 0.25; 0.5; 0.75; 1 wt% GnP was used. Dried PA 6 granulates (80°C; 4 hours) were mechanically mixed with the reinforcing materials for two minutes, and every 5 minutes it was remixed for 10 seconds to avoid settling, then extruded and granulated (particle size: 4.5 mm). Dumbbell type specimens (1A type according to the ISO 527-2 standard) were injection molded on an Aurburg Allrounder Advance 370S 700-290

injection molding machine. The injection molding temperature was 275°C and the maximal pressure was 800 bar. The mold temperature was set to be 80°C.

*2.3. Characterization methods*

Before the mechanical tests, the specimens were conditioned 50% relative humidity at room temperature for a month than the temperature was set to be 25°C (beside the 50% relative humidity) for a further week. Tensile tests were performed on a Zwick Z020 universal testing machine according to EN ISO 527. The crosshead speed was 5 mm/min during tensile tests and 5 specimens were tested from each material.

The applied tensile speed influences the measured strength of polymers and polymer matrix composite. This is especially true for thermoplastic polymers. As at fatigue tests the tensile speed changes relatively fast, high speed tensile tests has to be carried out to assess a strength value in the test speed region where the fatigue tests are performed. Based on former experiments crosshead speed of 200 mm/min was chosen for high speed tensile tests and the results were the references to determine the load levels for fatigue tests. At this test also 5 specimens were tested from each material.

Fatigue tests were carried out on an Instron 8872 hydraulic tensile testing machine equipped with Instron 2742-301 type hydraulic grips. The tests were performed on 5 specimens for each load level. The load-controlled fatigue tests were performed under tension-tension load with sinusoidal waveform. The excitation frequency was 2 Hz in each cases and the load factor was R=0.1 (R=minimum stress/maximum stress). The test finished when the specimen was broken or necking started. The temperature of the specimen surface was measured with a FLIR A325sc infrared camera. During the tests, the area of the whole surface was inspected and the highest temperature was registered.

The fibers were burned out from matrix at 600°C for 1 hour, after the recovery the fibers length was measured by Olymus BX51 optical microscope. Fiber length distribution was determined from length data of ca. 1000 fibers.

The fracture surfaces of the broken tensile and fatigue tested specimens were investigated with a Jeol 6380 LA type scanning electron microscope (SEM) after sputtering them with a thin gold layer. Picture from perpendicular direction to the tensile axis was also made to determine the protruding length of the fibers. To determine the length histogram at least 150 fiber were measured.

## 3. Results and discussion

### *3.1. Tensile properties*

The results of the tensile tests showed that in case of nanocomposites the presence of graphene did not cause a significant change in the tensile strength. Although in case of lower nanoparticle contents a moderate increment is noticeable, at higher contents the tensile strength showed lower values compared to the matrix material (Table 1.). The same tendency could be observed for the Young's moduli. Elongation at break also decreased with the increasing filler content, hence the material behaved in a more rigid way in the presence of graphene. These results refer to inappropriate graphene dispersion in the matrix.

As it was expected, basalt fiber increased tensile strength significantly. In case of hybrid composites, there was no significant change in strength compared to the basalt fiber reinforced one, but graphene notably enhanced Young's modulus, and that refers to better nanoparticle dispersion.

Table 1: Tensile properties of nano and hybrid composites.

| Material | Tensile strength [MPa] | Young's modulus [MPa] | Elongation at break [%] |
|---|---|---|---|
| PA 6 | 56.9 ± 0.7 | 2054 ± 17 | 58.8 ±15.5 |
| PA 6 / 0.25 GnP | 59.8 ± 0.6 | 2244 ± 37 | 20.3 ± 3.4 |
| PA 6 / 0.5 GnP | 57.5 ± 0.9 | 2259 ± 30 | 11.9 ± 2.7 |
| PA 6 / 0,75 GnP | 56.0 ± 0.9 | 2220 ± 28 | 10.9 ± 2.3 |
| PA 6 / 1 GnP | 53.0 ± 2.0 | 2123 ± 28 | 12.1 ± 3.7 |
| PA 6 / 30 BF | 99.0 ± 0.3 | 4419 ± 154 | 5.1 ± 0.1 |
| PA 6 / 30 BF/ 0.25 GnP | 101.6 ± 0.9 | 4917 ± 24 | 4.8 ± 0.2 |
| PA 6 / 30 BF/ 0.5 GnP | 99.9 ± 0.2 | 4902 ±124 | 4.7 ± 0.2 |
| PA 6 / 30 BF/ 0.75 GnP | 95.8 ± 0.7 | 4872 ± 108 | 4.5 ± 0.2 |
| PA 6 / 30 BF/ 1 GnP | 94.1 ± 0.6 | 4858 ± 82 | 4.4 ± 0.1 |

In order to examine if nanoparticle dispersion was successful, scanning electron microscope images were prepared from the fracture surfaces. Large aggregates could be found on the surface of nanocomposites (Fig 1. a, b), the average aggregate size was 75 µm. At higher graphene content only the number of aggregates increased but their size did not change. The results indicated unambiguously that theses aggregated particles were the starting points of fracture. In case of BF reinforced composites (Fig. 1. c) the characteristic failure form is fiber breakage, but fiber pull-out can also be observed. Nevertheless, adhesion between the matrix and the reinforcing material is strong enough, reflected in the enhanced tensile properties. In case of hybrid composites such large aggregates could not be found. As it was expected, the presence of micro-fibers helped to break up the large nanoparticle aggregates, and this way better dispersion could be achieved (Fig 1. c).

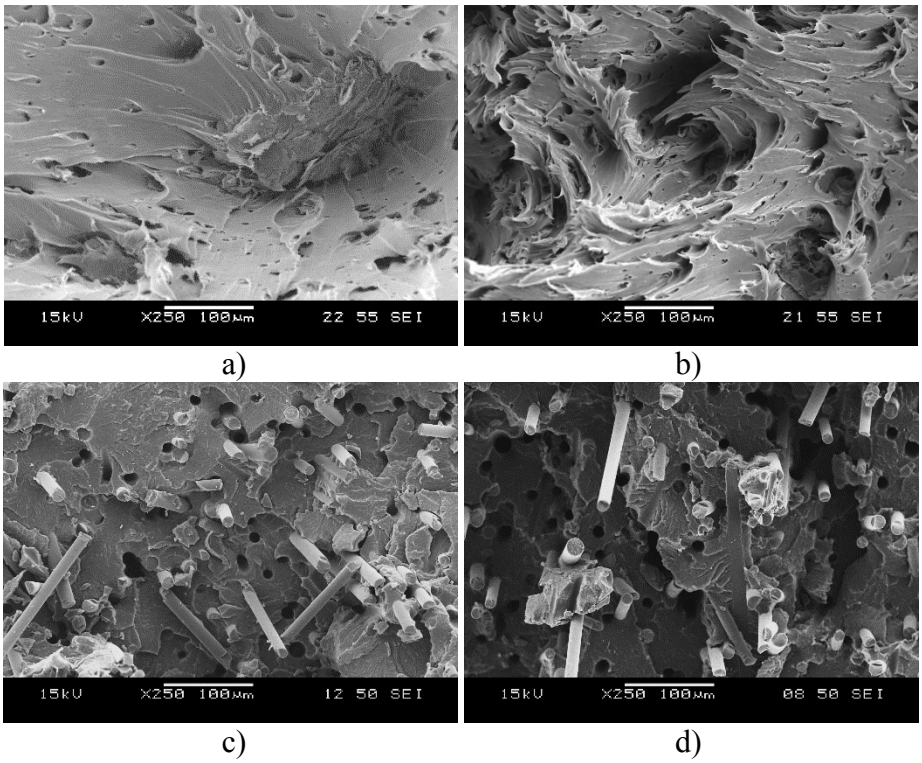


Figure 1. Fracture surfaces of tensile tested composites: a) PA6 / 0.25 GnP; b)PA6 / 0.75 GnP; c) PA 6 / 30 BF, d) PA 6 / 30 BF / 0.25 GnP

The positive effect of nanoparticles on the Young's moduli and the on strength at 0,25 graphene content could be explained even by better fiber-matrix bonding or the stress distribution effects of the nanoparticles. To decide which effect was dominant the fracture surfaces of tensile tested specimens were investigated. The measurement of protruding length of the fibers on the fracture surface is a feasible way to compare the evolved fiber-matrix adhesion at different composites as Vas et al. [38] showed. Figure 2 a shows the fiber length distributions of fiber length at 30 wt% basalt fiber containing composite and its 0.25 wt% GnP containing hybrid. It can be concluded that that there were no significant difference between the micro and hybrid composites fiber length after injection molding, that is why the protruding length can compared in case of these composites. The average protruding length (Figure 2 b) of the fibers were close to each other at the examined composites; the mean values were 104+-40 µm and 104+-36 µm. Based on these results it can be stated, that the presence of graphene did not affected the fiber-matrix bonding.

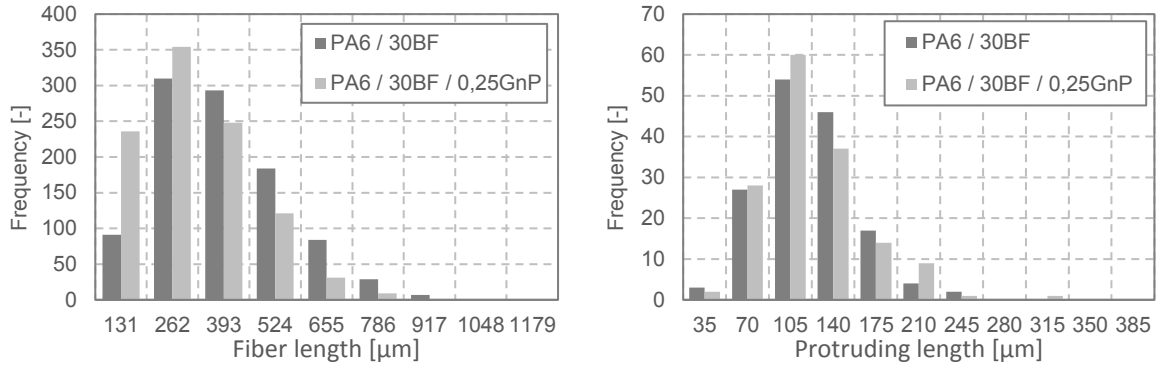


a) b)

Figure 2. Histogram of fiber length after injection molding (a) and protruding length of fibers on the fracture surface (b)

*3.2. Fatigue tests*

In this study the low-cycle fatigue behavior of the materials is revealed. Low-cycle means that relatively high loads are applied during the tests (Table 2.). The tensile strength ($\sigma_{max}$) measured at the crosshead speed of 200 mm/min for polyamide 6 was used as a reference to calculate the maximum stresses of different load levels for the PA 6 and its nanocomposites, and the tensile strength of basalt fiber reinforced composite was chosen for the PA 6 / BF and its hybrids.

Table 2: Load levels and applied stresses during fatigue tests in case of polyamide 6, nano and hybrid composites.

| | $\sigma_{max}$ [MPa] | 90% $\sigma_{max}$ [MPa] | 80% $\sigma_{max}$ [MPa] | 75% $\sigma_{max}$ [MPa] | 70% $\sigma_{max}$ [MPa] |
|---|---|---|---|---|---|
| PA 6 and nanocomposites | 51.3 | 46.2 | 41.0 | 38.5 | 35.9 |
| PA 6 / BF and hybrids | 107.9 | 97.1 | 86.3 | - | 75.5 |

In case of PA 6 and its nanocomposites necking, while in case of composites with BF content fracture meant the end of the fatigue test. Fig. 3 shows the stress-number of cycles (S-N) curve for neat PA 6. As it was expected, fatigue life was higher at lower load levels. The change was the most significant between 75% and the 70% load levels, where the cycles to failure increased from 400 to 23500.

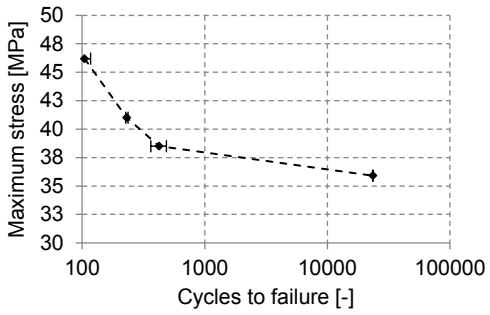


Figure 3. S-N curve for polyamide 6

To examine the structure-property relationships during fatigue tests, the instantaneous elongation and the maximum temperature of specimens were registered in each cycle. Figure 4 shows the elongation - determined as the ratio of specimen deformation at the mean stress value and the initial length in each cycle - and the temperature of neat PA 6 specimens as a function of cycle number measured at 70% load level. In the first period temperature and elongation increased relatively fast (between 100 and 500 cycles). Afterwards temperature stabilized at a nearly constant value, and deformation increased less intensively.

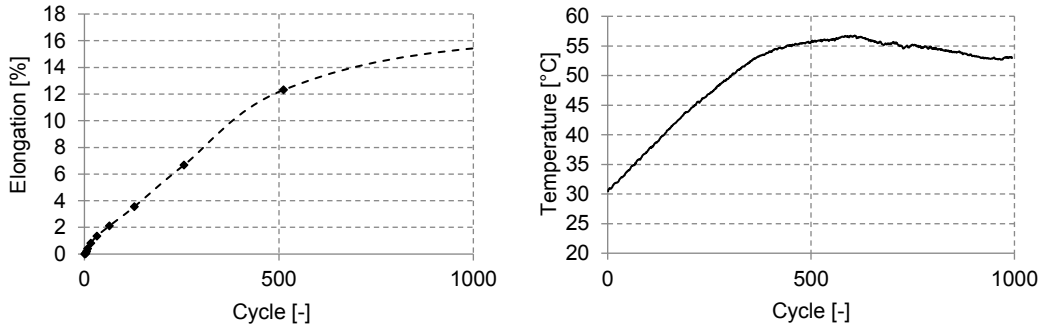


Figure 4. Elongation and temperature change during fatigue test at 35.9 MPa maximum stress in case of polyamide 6 samples

The temperature increment in the first period can be explained by the well-known good damping and poor thermal conductivity of PA 6. At around glass transition temperature the mobility of molecules increases, and that means heat can be transported more effectively from the critical areas, as a result nearly constant temperature can be achieved. This process was not observed at higher load levels because of the higher amplitudes, and this larger deformation

generated more heat, i.e. faster temperature increment, therefore faster failure processes were detected (Fig 5. a.). From the aspect of temperature increase, the presence of the nanoparticles did not change the values but the failure process was slightly longer (Fig 5. b.).

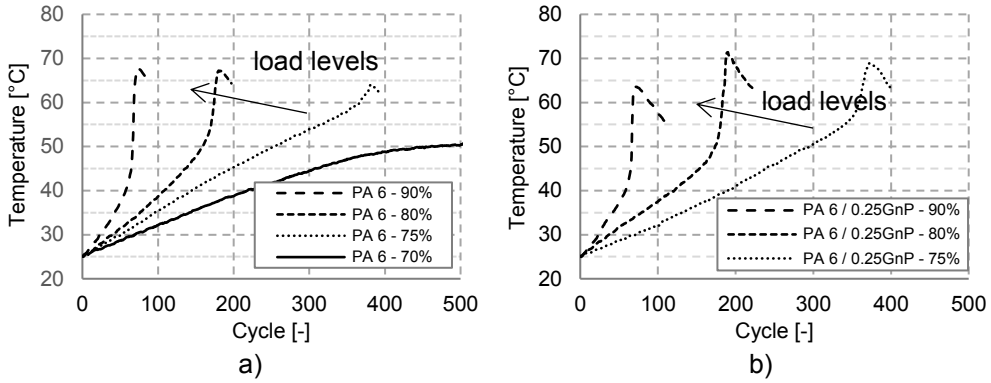


Figure 5. Temperature change during fatigue tests at different load levels in case of polyamide 6 (a) and nanocomposites (b)

The temperature increment at basalt fiber reinforced composites was also observed but compared to the neat matrix or the nanocomposites, it was less remarkable (Fig 6.). At the moment of failure temperature suddenly increases since during crack propagation the energy stored in the elastic deformation components is released, and a new surface is created with its help. This process involves a considerable heat release. In case of hybrid composites with 0.25 wt% GnP content, the temperature as a function of cycle number did not change compared to the case of microcomposites at the same load levels. Similarly to the nanocomposites, the failure process was also longer in case of hybrid materials (Fig. 6. b.). The same tendency was observed in case of hybrids with higher nanoparticle content.

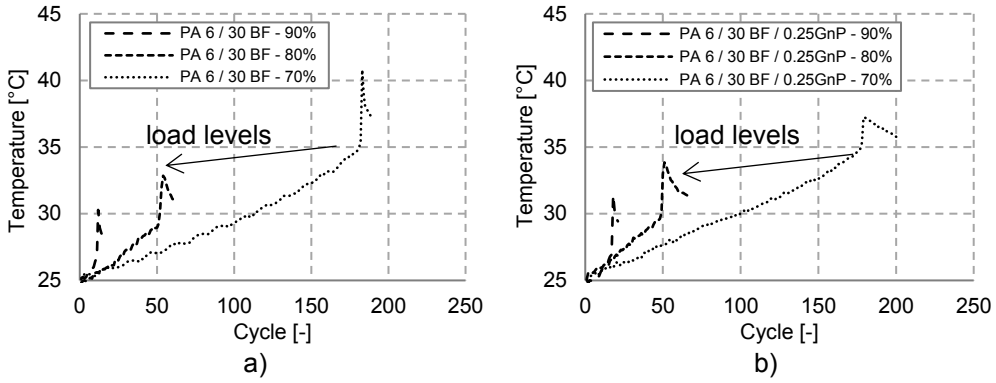


Figure 6. Temperature change during fatigue tests at different load levels in case of basalt fiber reinforced (a) and hybrid composites with 0.25 GnP content (b)

For nanocomposites the cycle number connected to failure significantly decreased as nanoparticle content increased (Fig.7. a., Table 3.). This effect can be explained by the imperfect nanoparticle dispersion that is also revealed by the tensile investigations (Fig. 1. a). The elongation of specimens during fatigue tests was smaller at low graphene contents compared to the values measured in case of neat polyamide 6 (Fig. 7. b). The effect was more outstanding for the nanocomposite with 0.25 wt% GnP content, where the measured values were only fractions of the elongation of the reference material. This means that cyclic creep decreased, a very important feature from an engineering design point of view. This effect correlates with our previous results where graphene increased the modulus of elasticity of composites and decreased the residual deformation at wide range of tensile loads [32].

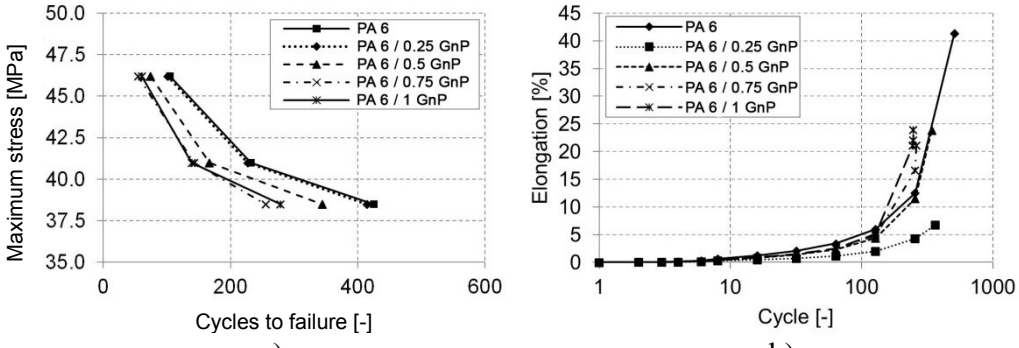


Figure 7. S-N curves (a) and elongation (b) of nanocomposites

Table 3: Composites and hybrid composites fatigue life (number of cycles survived until failure).

| Load [%] | PA 6 | PA 6 / 0,25 GnP | PA 6 / 0, 5GnP | PA 6 / 0,75 GnP | PA 6 / 1 GnP |
|---|---|---|---|---|---|
| | cycle [-] | cycle [-] | cycle [-] | cycle [-] | cycle [-] |
| 90 | 105 ± 13 | 102 ± 7 | 74 ± 10 | 55 ± 27 | 60 ± 7 |
| 80 | 232 ± 5 | 227 ± 24 | 167 ± 7 | 143 ± 3 | 139 ± 3 |
| 75 | 426 ±62 | 414 ± 14 | 344 ± 17 | 256 ± 11 | 279 ± 24 |
| Load [%] | PA 6 / 30 BF | PA 6 / 30 BF / 0,25 GnP | PA 6 / 30 BF / 0,5 GnP | PA 6 / 30BF / 0,75 GnP | PA 6 / 30BF / 1 GnP |
| | cycle [-] | cycle [-] | cycle [-] | cycle [-] | cycle [-] |
| 90 | 18 ± 1 | 24 ± 1 | 18 ± 2 | 19 ± 2 | 16 ± 1 |
| 80 | 55 ± 4 | 75 ± 5 | 60 ± 3 | 61 ± 14 | 49 ± 3 |
| 70 | 175 ± 19 | 218 ± 7 | 187 ±4 | 151 ± 19 | 147 ± 12 |

During fatigue tests at the graphene containing monocomposites the appearance of necking was the visible proof that the structure of the specimen drastically changed thus the specimen reached its fatigue life. During the test the temperature increment was uniform in the whole specimen (Fig. 7. a.), until it reached the final part of the fatigue life. In this period the temperature increased in the area where the later the necking started. Figure 7 b. shows that before necking in a smaller region the temperature increased compared to the other part of the specimen.

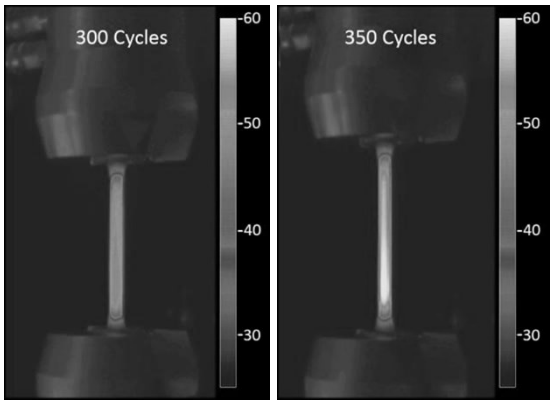


a) b)

Figure 7. PA6 / 0.25 GNP composites temperature during fatigue test at different cycle number, b) the increased temperature zone was the site where the necking started.

After the test at this region some blisters on the neck surface were observed (Fig. 8. a). At the blisters the specimens were cut with a sharp blade and the cross sections were investigated with SEM (Fig. 8. b). Under the examined surface of different samples relatively large graphene aggregates were found. This means that large aggregates are the starting points of the failure process which initialized by the higher deformations around this particle.

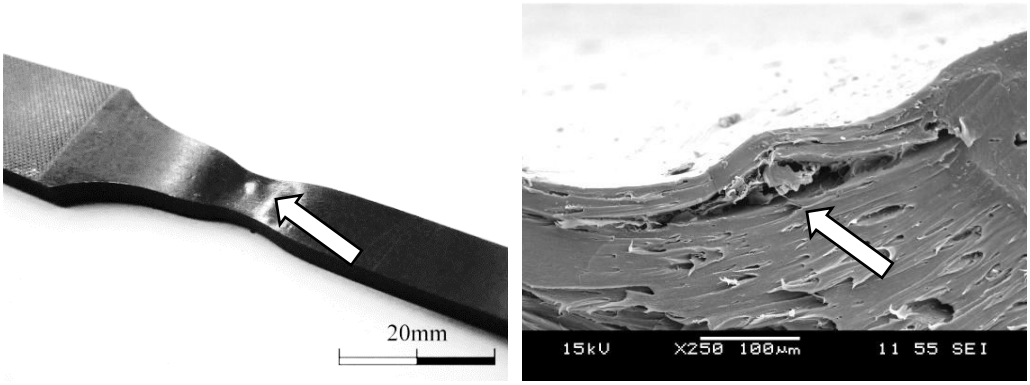


a) b)

Figure 8. A blister on the neck surface of specimen (marked with an arrow) (a), and a cut specimen cross section with a graphene aggregate under the surface (marked with an arrow) (b)

At low graphene contents the hybrid composites showed better fatigue properties compared to the reference basalt fiber monocomposite beside relatively low standard deviations. At 0.25 wt% graphene content 30% increment was experienced in the cycles to failure values at every load level (Fig 9. a, Table 3.). Over 0.5 wt% graphene content this positive effect was not found any more. At 0.25 wt% graphene content, besides the increment in the survived cycles, remarkable decrement in the cyclic creep values was revealed (Fig 9. b, Table 3.).

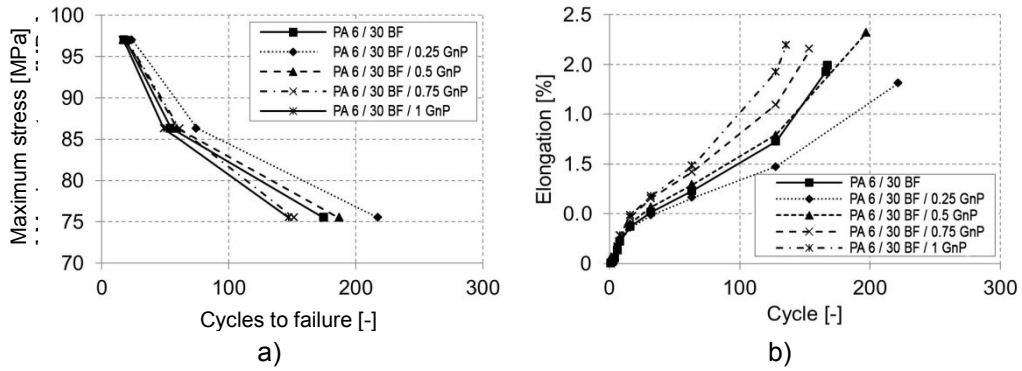


Figure 9. S-N curves and elongation of hybrid composites

To shed light on the structural causes of the enhanced fatigue life, the fracture surfaces were investigated by SEM. The evolved surfaces of hybrid composites were similar to that of basalt fiber reinforced composites as in case of all composite types the fracture surfaces can be divided into a micro ductile and a micro brittle part. Fig. 10 shows these two parts in case of PA6 / 30BF and hybrid composite with 0.25 wt% GnP content. Based on the results, it can be stated that crack propagation during fatigue tests was very similar in case of both material types, as it is also written by Horst *et al.* [23]. Firstly, the cracks appear at the end of fibers because they are stress concentration points, then the crack grows along fibers, and finally these areas of failure connect to each other and create voids. This tough breakage is dominant until a critical size is reached, when the test ends with a sudden and catastrophic rigid breakage. The presence of graphene did not change the failure process itself but it may slowed down crack propagation. This phenomenon can be explained by better load distribution effect of the nanoparticles.

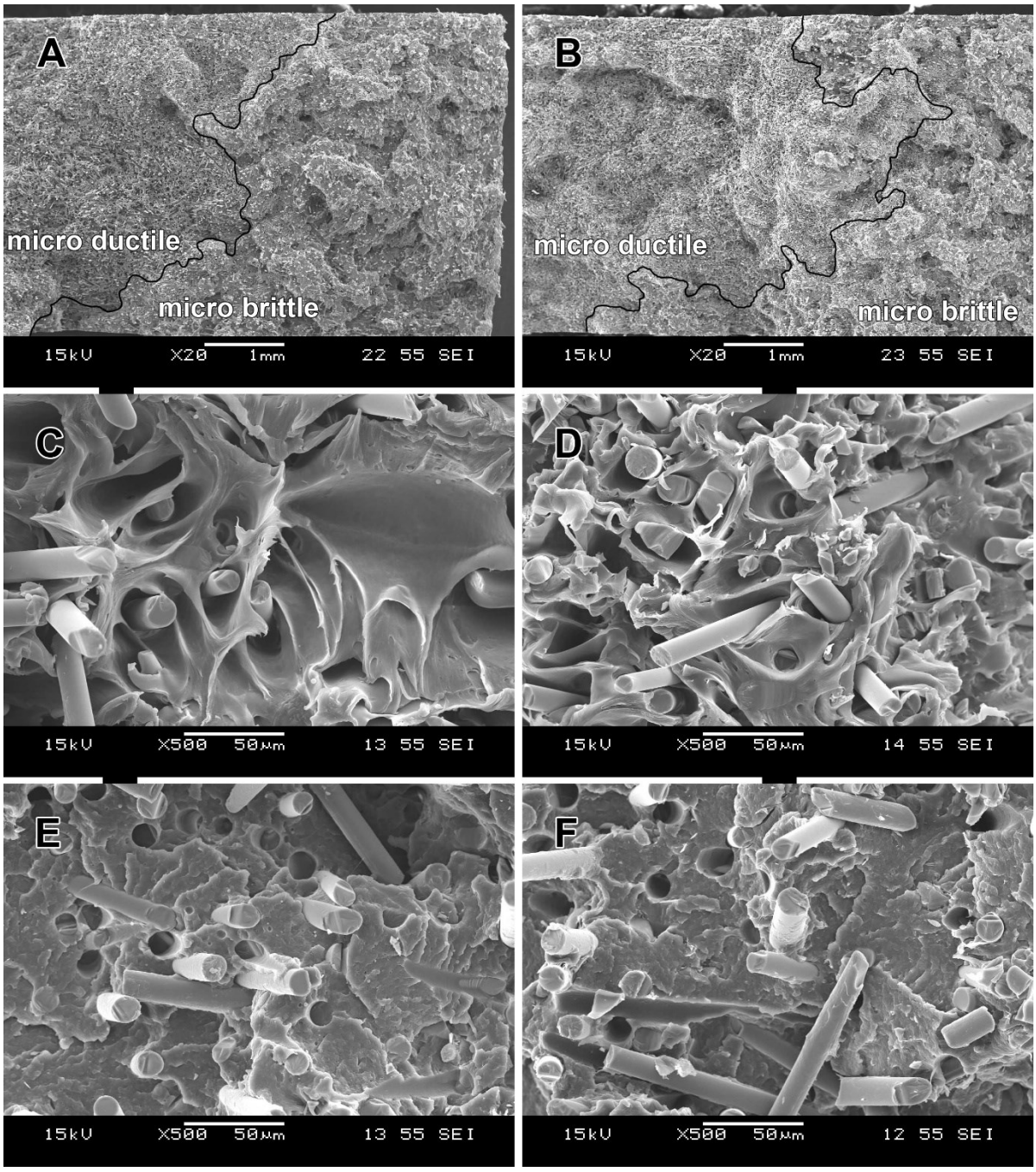


Figure 10. Typical fracture surface of the PA6/30BF composite (A, C, E) and hybrid composite with 0.25 wt% GnP content (B, D, F).

## 4. Conclusions

In this study PA 6 matrix nano and hybrid composites were extruded followed by injection molding. The tensile test results showed that the presence of graphene did not change the mechanical properties of composites significantly; however, in case of hybrid composites with low graphene contents some increment in the Young's modulus was exhibited. During low-cycle fatigue tests of nanocomposites with graphene content significant decrements in the fatigue life were observed. This can be explained by the high number of graphene aggregates that are observed in the SEM pictures of the cut surfaces of the specimens. In spite of the improper dispersion in nanocomposites with 0.25 wt% GnP content, the cyclic creep decreased significantly compared to the value of neat PA 6. A similar favorable effect was revealed in case of hybrid composites with 0.25 wt% GnP content, but in this case a remarkable increment in fatigue life was also exhibited at all applied load levels compared to the basalt fiber monocomposite.

## 5. Acknowledgements

This research was realized in the framework of TÁMOP 4.2.4.A/1-11-1-2012-0001 „National Excellence Program – Elaborating and operating an inland student and researcher personal support system". The project was subsidized by the European Union and co-financed by the European Social Fund. This research was also supported by the Hungarian Research Fund (OTKA PD105564).

## 6. REFERENCES

1. Kretsis G. A review of the tensile, compressive, flexural and shear properties of hybrid fiber-reinforced plastics. *Composites* 1974; 18: 13-23.

2. Harris B, and Bunsell AR. Hybrid carbon and glass fiber composites. *Composites* 1974; 5: 157-164.

3. Murugan R, Ramesh R, and Padmanabhan K: Investigation on static and dynamic mechanical proeprties of epoxy based woven fabric glass/carbon hybrid composite laminates, in: *12th Global Congress on Manufacturing and Management*, Vellore, India, 8-10 December 2014, paper no. GCMM-2014, pp.459-468

4. Juhász Z, and Szekrényes A. Progressive buckling of a simply supported delaminated orthotropic rectangular composite plate, *Int J Solids Struct* 2015; 69–70: 217-229.

5. Molnár K, Košťáková E, and Mészáros L. The effect of needleless electrospun nanofibrous interleaves on mechanical properties of carbon fabrics/epoxy laminates, *Express Polym Lett* 2014; 8: 62-72.

6. Turcsán T, and Mészáros L. Development and mechanical properties of carbon fibre reinforced EP/VE hybrid composite systems. *Period Polytech Mech* 2014; 58: 127-133.

7. Singh V, Joung D, Zhai L, et al. Graphene based materials: Past, present and future. *Prog Mater Sci* 2011; 56: 1178-1271.

8. Kuilla T, et al. Recent advances in graphene based polymer composites. Prog Polym Sci 2010; 35: 1350 -1375.

9. Paszkiewicz S, et al. Enhanced thermal and mechanical properties of poly(trimethylene terephthalate-block-poly(tetramethylene oxide) segmented copolymer based hybrid nanocomposites prepared by in situ polymerization via synergy effect between SWCNTs and graphene nanoplatelets, *Express Polym Lett 2015;* 9: 509-524.

10. Balandin AA, et al. Superior thermal conductivity of Single-Layer Graphene, *Nano Lett* 2008; 8: 902-907.

11. Lee C, et al: Measurement of the elastic properties and intrinsic strength of monolayer Graphene, *Science* 2008; 321: 385-388.

12. Marinho B, et al. Electrical conductivity of compacts of graphene, multi-wall carbon nanotubes, carbon black, and graphite powder. *Powder Technol* 2012; 221: 351-358.

13. Rafiee MA, et al. Enhanced Mechanical Properties of Nanocomposites at Low Graphene Content, *Polymer* 2009; 47: 4760-4767.

14. Rafiq R, et al. Increasing the toughness of nylon 12 by the incorporation of functionalized graphene. *Carbon* 2010; 48: 4309-4314.

15. Jin J, et al. Preparation and characterization of high performance of graphene/nylon nanocomposites, *Eur Polym J* 2013; 49: 2617-2626.

16. Mittal G, et al. A review on carbon nanotubes and graphene as fillers in reinforced polymer nanocomposites. *J Ind Eng Chem* 2015; 21: 11-25.

17. Nair KCM., et al. Rheological behavior of short sisal fiber-reinforced polystyrene composites. *Compos Part A-APPL S* 2000; 31: 1231-1240.

18. Binding DM. Capillary and contraction flow of long-(glass) fiber filled polypropylene. *Compos Manuf* 1991; 2: 243-252.

19. Mészáros L, et al. Preparation and mechanical properties of injection moulded polyamide 6 matrix hybrid nanocomposites. *Compos Sci Technol* 2013; 75: 22-27.

20. Wan T, et al. Multi-scale hybrid polyamide 6 composites reinforced with nano-scale clay and micro-scale short glass fibre. *Compos Part A-APPL S* 2013; 50: 31-38.

21. Bernasconi A, et al. Effect of fibre orientation on the fatigue behaviour of a short glassfibre reinforced polyamide-6. *Int J Fatigue* 2007; 29: 199-208.

22. Arif MF, et al. Multiscale fatigue damage characterization in short glass fiber reinforced polyamide-66. *Compos Part B-Eng* 2014; 61: 55-65.

23. Horst JJ, and Spoormaker JL. Fatigue fracture mechanisms and fractography of short-glassfibre-reinforced polyamide 6. *J Mater Sci* 1997; 32: 3641-3651.

24. Bernasconi A, Davoli P, and Armanni C. Fatigue strength of a clutch pedal made of reprocessed short glass fiber reinforced polyamide. *Int J Fatigue* 2010; 32: 100-107.

25. Launay A, et al. Cyclic behaviour of short glass fiber reinforced polyamide: Experimental study and constitutive equations. *Int J Plasticity* 2011; 27: 1267-1293.

26. Banaarbia et al. Influence of relative humidity and load frequency on the PA6.6 cyclic thermomechanical behavior: Part I. mechanical and thermal aspects. *Polym Test* 2014; 40: 290-298.

27. Esmaeillou B, et al. Multi-scale experimental analysis of the tension-tension fatigue behavior of a short glass fibre reinforced polyamide composite. *11th International Conference on the Mechanical Behaviour of Materials*, Milano, Italy, 5-9 June 2011, paper no. ICM11. pp. 2117-2122.

28. Ramkumar A, and Gnanamoorthy R. Axial fatigue behaviour of polyamide-6 and polyamide-6 nanocomposites at room temperature. *Compos Sci Technol* 2008; 68: 3401-3405.

29. Loos MR, et al.: Enhanced fatigue life of carbon nanotube-reinforced epoxy composites. *Polym Eng Sci* 2012; 52: 1882-1887.

30. Grimmer CS, and Dharan CKH. Enhancement of delamination fatigue resistance in carbon nanotube reinforced. *Compos Sci Technol* 2010; 70: 901-908.

31. Dai G, and Mishnaevsky L Jr. Carbon nanotube reinforced hybrid composites: Computational modeling of environmental fatigue and usability for wind blades. *Compos Part B-Eng* 2015; 78: 349-360.

32. Fenner JS, and Daniel IM. Hybrid nanoreinforced carbon/epoxy composites for enhanced damage tolerance and fatigue life. *Compos Part A-APPL S* 2014; 65: 47-56.

33. Yang L, et al. Interfacial shear behavior of 3D composites reinforced with CNT-grafted carbon fibers. *Compos Part A-APPL S* 2012; 43: 1410-1418.

34. Kornmann X, et al. Epoxy - layered silicate nanocomposites as matrix in glass fibre - reinforced composites. *Compos Sci Technol* 2005; 65: 2259-2268.

35. Hasque A, et al. S2-Glass/Epoxy Polymer Nanocomposites: Manufacturing, Structures, Thermal and Mechanical Properties. *J Compos Mater* 2003; 37: 1821-1837.

36. Zhiqi S, et al. The effects of Clay on fire performance and thermal mechanical properties of woven glass fibre reinforced polyamide 6 nanocomposites. *Compos Sci Technol* 2010; 70: 2063-267.

37. Mészáros L, and Szakács J. Elastic recovery at graphene reinforced PA 6 nanocomposites. In: *5th International Nanocon Conference*, Brno, Czech Republic, paper no. 1955 pp. 1-5.

38. Vas ML, Ronkay F, and Czigány T. Active fiber length distribution and its application to determine the critical fiber length. *Polym Test* 2009; 28: 752-759.